Experimental Determination of Activation Energies for Gas-Phase Ethyl and *n*-Propyl Cation Transfer Reactions†

Travis D. Fridgen*,‡ and Terry B. McMahon*,§

Department of Chemistry, University of Waterloo, Waterloo, Ontario N2L 3G1, Canada

Received: October 23, 2001; In Final Form: January 30, 2002

Alkyl cation transfer reactions between ethanol and protonated ethanol and ethanol and protonated propionitrile, as well as between *n*-propanol and protonated *n*-propanol have been investigated experimentally by low-pressure Fourier transform ion cyclotron resonance (FT-ICR) mass spectrometry. The two ethyl cation transfer reactions were found to be the dominant reaction channels with association being only a minor reaction pathway. The *n*-propyl cation transfer reaction was found to compete with the association pathway resulting in an approximately 50:50 mixture of protonated di-*n*-propyl ether and the proton-bound dimer of *n*-propanol, depending on temperature and pressure. The enthalpies of activation were determined to be -16.1 ± 0.8, -17.5 ± 0.8, and -15.7 ± 0.9 kJ mol^{-1} for the ethanol/protonated ethanol, ethanol/protonated propionitrile, and *n*-propanol/protonated *n*-propanol alkyl cation transfer reactions, respectively. The entropies of activation were found to be essentially the same, -121 ± 28 J K^{-1} mol^{-1}, for all three reactions. All experimentally determined thermochemical properties agreed very well with those calculated at the MP2/6-31+G(d)//B3LYP/6-31+G* level of theory. Furthermore, the enthalpies and entropies of activation for the methy, ethyl, and *n*-propyl cation transfer reactions between the neutral alcohols and the respective protonated alcohols were found to be the same within experimental uncertainty.

1. Introduction

The study of ion/molecule reactions at very low pressures (10^{-9}−10^{-6} mbar) at which photon emission from the nascent ion/molecule complex is a viable means for stabilization has been quite successful in developing an understanding of ion/molecule interactions and the unimolecular processes that occur under these conditions. Several studies have been conducted, yielding rates of photon emission and lifetimes for nascent ion/molecule complexes with internal energies equal to the ion−neutral binding energy.[1,2] Through the use of master equation modeling of the rate constants for unimolecular dissociation of the nascent ion/molecule complex, accurate binding energies have been obtained for various systems.[3] We have studied the temperature dependence of the radiative association reaction for dimethyl ether and protonated dimethyl ether and have shown that the initial complex formed in the entrance channel is one in which a methyl group of the protonated dimethyl ether is complexed to the oxygen of the neutral dimethyl ether.[2] This methyl-bound complex then either rearranges to the proton-bound dimer or is the direct precursor for methyl cation transfer. At the low pressures of Fourier transform ion cyclotron resonance (FT-ICR) studies, the methyl cation transfer reaction, which eliminates methanol to yield trimethyloxonium ion, was also observed.[4] This S_N2 reaction becomes the dominant route at higher temperatures. The S_N2 channel is difficult to observe at higher pressures, such as in a high-pressure source, because third-body stabilization of the proton-bound dimer dominates. From the temperature dependence of the rate constant for methyl cation transfer, an experimental energy barrier, which lies 3.9 ± 1.2 kJ mol^{-1} above the energy of the reactants ($\Delta H^{\ddagger} = -1.1 \pm 1.2$ kJ mol^{-1}), was obtained.[4]

More recently, the thermochemistry pertaining to the transition state for the S_N2 reactions between neutral methanol and protonated methanol, protonated acetonitrile, and protonated acetaldehyde from temperature-dependent rate constants has been investigated.[5] These experimental barrier heights were found to agree quite well with those predicted by ab initio electronic structure calculations.

Work on elucidating thermochemical parameters for the transition state of S_N2 reactions has also been conducted by Mayer and co-workers.[6,7] From an examination of the metastable dissociation of proton-bound methanol/acetonitrile[6] and ethanol/acetonitrile[7] dimers and use of Rice−Ramsperger−Kassel−Marcus (RRKM) theory to model the kinetics of water loss, the barrier for isomerization of the proton-bound dimer to a water-complexed species (eq 1) was estimated.

$$[ROH\cdots H\cdots NCCH_3]^+ \rightarrow [RNCCH_3\cdots H_2O]^+ \qquad (1)$$

This isomerization barrier is the bottleneck for the S_N2 reaction because the water loss from protonated acetonitrile and neutral alcohols is exothermic. This is shown schematically in Figure 1. In the metastable dissociation experiments,[6,7] the proton-bound dimer (**I** in Figure 1) is prepared in the source and both the separated monomers (reactants) and the water-loss products are observed. In their RRKM calculations, the isomerization barrier (energy difference between **I** and **IV** in Figure 1) is fitted to obtain the appropriate rate constant for formation of products on the time scale of the metastable dissociation. McCormack and Mayer[8,9] have also recently measured rate constants for S_N2 reactions, at ambient temperature, within the confines of a quadrupole ion trap. From the rates of disappearance of the protonated monomers (alcohols or acetonitrile), the rate con-

† Part of the special issue "Jack Beauchamp Festschrift".

* To whom correspondence should be addressed.
‡ tdfridge@sciborg.uwaterloo.ca.
§ mcmahon@sciborg.uwaterloo.ca.

10.1021/jp013874w CCC: $22.00
Published on Web 03/30/2002

stants for the S_N2 reactions are obtained. RRKM modeling is performed with the energy barrier for isomerization as a variable, which leads to a determination of the barrier height.[8,9]

In the present work, with the use of methods described previously,[4,5] the reactions of protonated alcohols and neutral alcohols are examined and the rate constants for alkyl cation transfer are measured directly at low pressures in the FT-ICR cell. From the temperature dependence of the rate constants, the thermodynamic parameters for the S_N2 energy barrier are obtained directly as described below.

Data are obtained here for ethyl and *n*-propyl cation transfer reactions. The results of work on three S_N2 reactions, two ethyl cation transfer reactions of ethanol with protonated ethanol (eq 2) and protonated propionitrile (eq 3) and the *n*-propyl cation transfer reaction between *n*-propanol and protonated *n*-propanol (eq 4) are presented.

$$CH_3CH_2OH_2^+ + CH_3CH_2OH \rightarrow (CH_3CH_2)_2OH^+ + H_2O \quad (2)$$

$$CH_3CH_2CNH^+ + CH_3CH_2OH \rightarrow CH_3CH_2CNCH_2CH_3^+ + H_2O \quad (3)$$

$$CH_3CH_2CH_2OH_2^+ + CH_3CH_2CH_2OH \rightarrow (CH_3CH_2CH_2)OH^+ + H_2O \quad (4)$$

The experimental thermochemistries derived from these experiments are compared with those calculated by electronic structure calculations.

2. Experimental Procedure

All experiments were carried out with a Bruker CMS 47 FT-ICR mass spectrometer equipped with a 4.7 T magnet. Samples of ethanol (100%, Consolidated Alcohols), propionitrile (99%, Aldrich), and *n*-propanol (99.7%, Aldrich) were degassed using a minimum of three freeze−pump−thaw cycles and were introduced into the ICR cell via heated precision leak valves. The pressure inside the vacuum chamber was measured with a calibrated ionization gauge via a procedure described previously.[2,5] The calibration of the ion gauge for the pressure of ethanol was performed by measuring the rate of the self-protonation reaction in eq 5.

$$CH_3CH_2OH^{+\bullet} + CH_3CH_2OH \rightarrow C_2H_5O^{\bullet} + CH_3CH_2OH_2^+ \quad (5)$$

The reaction was monitored at three pressures ranging from 5.9×10^{-9} to 1.3×10^{-8} mbar (uncalibrated). The pressures obtained from the pseudo-first-order decay kinetics of the ethanol radical cation were compared with the collision rate constant calculated by the method of Su and Chesnavich.[10] A calibration factor of 1.50 ± 0.05 was obtained for the pressure of ethanol for which the reported error is a minimum value, reflecting only the standard deviation in the measurements and not the error associated with the calculated collision rate. In a similar fashion, the calibration factor for *n*-propanol was determined to be 1.25.

For each reaction investigated, the pressure of neutral ethanol or *n*-propanol was varied between calibrated pressures of 1.0×10^{-8} and 1.0×10^{-7} mbar. For reaction 3, the pressure of propionitrile was between 0.5 and 2.5 times that of ethanol.

The pulse sequence used for these studies is shown in Figure 2. Ionization was effected directly inside the ICR cell using

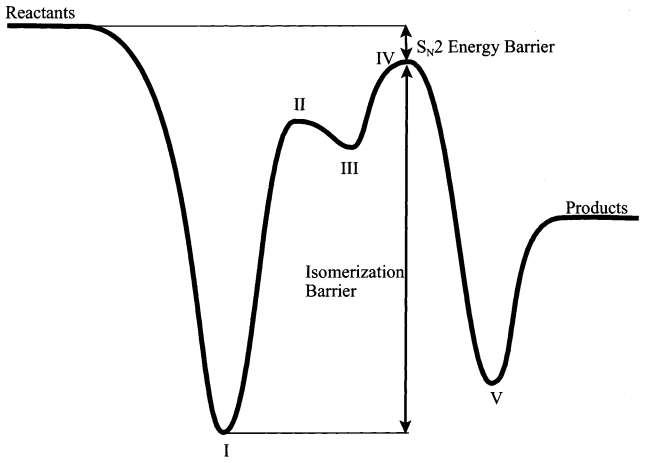

Figure 1. Reaction profile for a typical gas-phase S_N2 reaction involving alkyl cation transfer between a protonated and neutral reactant.

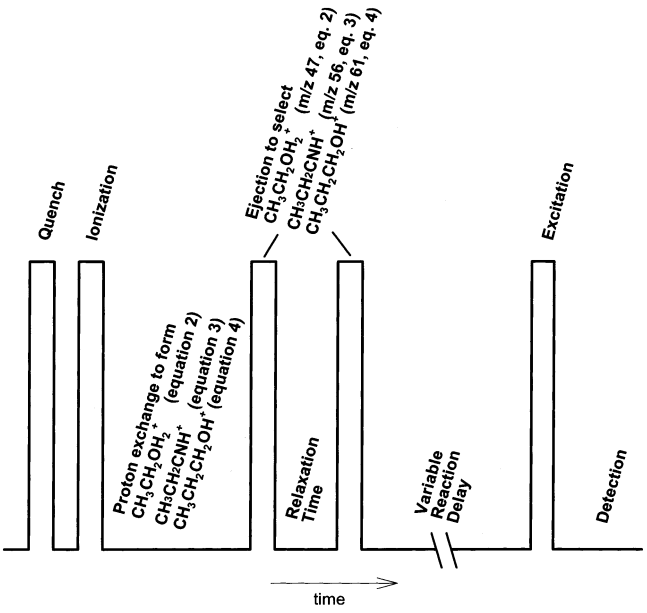

Figure 2. Scan function for the FT-ICR experiments reported in this work.

~100 ms pulses of 70 eV electrons. The first delay after ionization is incorporated into the experiment to produce either $CH_3CH_2OH_2^+$ (*m*/*z* 47), $CH_3CH_2CNH^+$ (*m*/*z* 56), or CH_3CH_2-$CH_2OH_2^+$ (*m*/*z* 61) by a series of proton-transfer reactions to the neutral precursor, after which all of the ions except the desired ionic precursor were ejected from the ICR cell by standard radio frequency (rf) ejection techniques. A second delay was incorporated to ensure thermal equilibrium of the ions. After this second delay, the ionic precursor of interest was once again isolated.

The intensities of the precursor and product ions (including ^{13}C contribution) were monitored typically until about 90% depletion of the precursor. The rate constants of methyl cation transfer for reactions 2−4 were obtained from a least-squares fitting of a semilogarithmic plot of normalized precursor ion intensity vs time. A typical mass spectrum for the reaction of protonated ethanol with ethanol to form protonated diethyl ether and water is shown in Figure 3 after 10 and 100 s for the reaction carried out at 294 K and a partial pressure of ethanol of 9.9×10^{-9} mbar. The corresponding semilogarithmic plot of ion intensities vs time is shown in Figure 4.

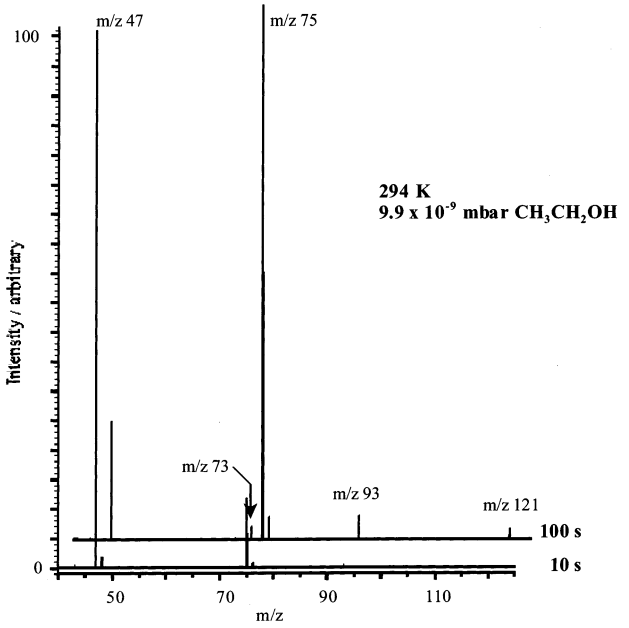

Figure 3. Mass spectra taken after delays of 10 and 100 s of reaction between protonated ethanol (*m*/*z* 47) and neutral ethanol conducted at 294 K and an ethanol pressure of 9.9×10^{-9} mbar. Note that the spectrum taken at 100 s is offset slightly to higher mass for clarity.

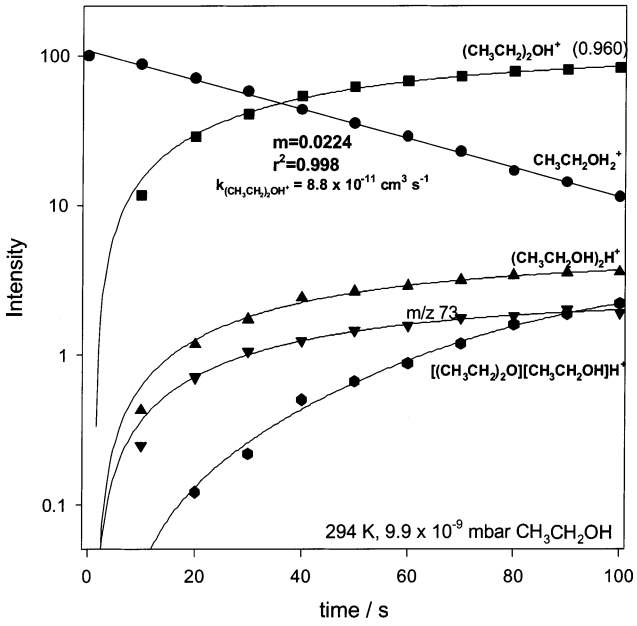

Figure 4. Semilogarithmic plot of intensity vs time for the reaction of protonated ethanol with neutral ethanol. The temperature and pressure conditions are the same as those in Figure 3.

3. Ab Initio Calculations

All electronic structure calculations were performed at the B3LYP and MP2 levels of theory in conjunction with the 6-31+G(d) basis set using the Gaussian 98 suite of programs.[11] Vibrational frequencies were calculated for the structures optimized at the B3LYP/6-31+G(d) level and basis set. Structure optimizations were also done using MP2/6-31+G(d). The frequency calculations at the B3LYP/6-31+G(d) level were used to correct the MP2/6-31+G(d) electronic energies for thermal energy contributions. Calculations were also performed at the G3(MP2) level of theory for the methyl cation exchange reactions to compare with the MP2/6-31+G(d)//B3LYP/6-31+G(d) calculations. Transition-state structures were verified by the presence of a single imaginary vibrational frequency corresponding to the vibrational mode in the correct reaction coordinate.

4. Data Analysis and Arrhenius Theory

According to Arrhenius theory, the rate constant of a chemical reaction varies with temperature according to the Arrhenius equation

$$\ln k = \ln A - \frac{E_a}{RT} \tag{6}$$

where k is the rate constant, A is the preexponential or frequency factor, E_a is the activation energy, and T and R are the Kelvin temperature and gas constant (8.314 J K^{-1} mol^{-1}), respectively. Thus from the slope, m, of a plot of ln k vs $1/T$, E_a and $\Delta H^{\ddagger}$, the activation energy and enthalpy of activation, respectively, can be obtained according to eqs 7 and 8, respectively,

$$E_a = -mR \tag{7}$$

$$\Delta H^{\ddagger} = E_a - 2RT \tag{8}$$

From the thermodynamic formulation of transition-state theory, the intercept of the Arrhenius plot, A, can be written in terms of the $\Delta S^{\ddagger}$,

$$A = \frac{k_B T}{h} e^2 e^{\Delta S^{\ddagger}/R} \tag{9}$$

where k_B is the Boltzmann constant. Therefore, from the intercept of the Arrhenius plot, $\Delta S^{\ddagger}$ can be determined. The errors in the rate constants represent only the standard deviation of the average rate constant, measured at various pressures, at each temperature. The slopes and intercepts as well as the error were calculated using a least-squares regression in which each point was weighted by the standard deviation in each point on the Arrhenius plot. These errors therefore reflect only random error and not systematic errors. The possibility of a slightly incorrect temperature within the ICR cell affects the absolute rate constant but has little effect on the temperature-dependent values reported here. For example, a 5 K difference in temperature between the reported values and actual values would only result in a 0.5 kJ mol^{-1} difference in E_a and a 1 J K^{-1} mol^{-1} difference in $\Delta S^{\ddagger}$.

5. Results and Discussion

5.1. Mass Spectra, Rate Constants, and Arrhenius Plots. *$CH_3CH_2OH_2^+$ + CH_3CH_2OH.* The primary product in the reaction between ethanol and protonated ethanol at all temperatures studied is protonated diethyl ether at *m*/*z* 75 as seen in Figure 3. Other products include the proton-bound dimer of ethanol at *m*/*z* 93 and the proton-bound dimer of ethanol and diethyl ether at *m*/*z* 121. These two proton-bound dimers are not totally unexpected, although their stabilization at such low pressures likely requires that there be some radiative stabilization (photon emission) occurring along with collisional stabilization. Although too little proton-bound dimer is observed to accurately obtain information from the radiative association of the proton-bound dimer of ethanol, the radiative association of the mixed proton-bound dimer of ethanol and diethyl ether is sufficiently significant that it can be studied. This reaction is considered in a separate manuscript.[12]

TABLE 1: Rate Constants for the Ethyl Cation Exchange Reaction between Ethanol and Protonated Ethanol

temp, K	rate constant[a]	temp, K	rate constant[a]
294	8.6 ± 0.3	322	5.7 ± 0.2
301	7.4 ± 0.3	327	5.4 ± 0.3
309	6.6 ± 0.3	335	4.7 ± 0.2
310	6.3 ± 0.2	340	4.6 ± 0.2
317	6.0 ± 0.2		

[a] Rate constants in units of 10^{-11} cm^3 s^{-1}.

Also observed in the mass spectra is an ion at *m*/*z* 73. This is most likely O-ethylated acetaldehyde. This product appears even when the ion gauge is turned off and, therefore, is not due to pyrolysis of ethanol in the ion gauge. The presence of *m*/*z* 73 can only be ascribed to loss of H_2 from nascent *m*/*z* 75,

$$CH_3CH_2OH_2^+ + CH_3CH_2OH \rightarrow \underset{m/z\ 75}{(CH_3CH_2)_2OH^+} + H_2O$$

$$\underset{m/z\ 73}{(CH_3CH_2)_2OH^+}{}^* \rightarrow CH_3CH_2O{=}CHCH_3^+ + H_2 \quad (10)$$

which is about 7.5 kJ mol^{-1} endothermic[13] from reactants and explains why *m*/*z* 73 is only present in small amounts, ~1%. The loss of H_2 from protonated methylamine, methanol, and methyl fluoride has been studied by metastable ion mass spectrometry and ab initio theory.[14] The barrier for H_2 loss from these three reactants was found to be significant from the kinetic energy releases measured and from ab initio theory. Therefore, the energy requirement for the loss of H_2 in eq 10 is likely to be greater than 7.5 kJ mol^{-1}.

The rate constants for formation of protonated diethyl ether from ethanol and protonated ethanol are given in Table 1 at various temperatures ranging from 294 to 340 K. McMahon and Beauchamp[15] measured a rate constant for this reaction of 24 × 10^{-11} cm^3 s^{-1} (296 K), while Karpas and Meot-Ner[16] obtained a value of 6.8 × 10^{-11} cm^3 s^{-1} (340 K), both in ICR mass spectrometers. McCormack and Mayer[8] obtained a value of 14 × 10^{-11} cm^3 s^{-1} in a quadrupole ion trap. The differences among these values can likely be attributed to the uncertainty in the neutral pressures.

The logarithms of the rate constants are plotted against inverse pressure (Arrhenius plot) in Figure 5. From the slope of this plot, E_a and $\Delta H^{\ddagger}$ were determined to be −11.1 ± 0.8 and −16.1 ± 0.8 kJ mol^{-1}, respectively. The energy barrier estimated by McCormack and Mayer[9] from their ion trap studies was −5 ± 8 kJ mol^{-1}, which is in reasonable agreement with our purely experimental value.

From the intercept, a $\Delta S^{\ddagger}$ of −121 ± 27 J K^{-1} mol^{-1} was obtained. It should be noted that the ion gauge calibration factors would have no effect on the activation energies obtained via the Arrhenius analysis, but the entropy of activation is dependent on the calibration factor. This effect will be discussed further below.

$CH_3CH_2CNH^+ + CH_3CH_2OH$. The primary product observed in the reaction of protonated propionitrile and ethanol was *N*-ethylated propionitrile cation at *m*/*z* 84 (eq 3). The only other products observed were the proton-bound dimer of propionitrile (*m*/*z* 111) and the mixed propionitrile/ethanol proton-bound dimer *m*/*z* (102). These two minor products varied in abundance, as expected, depending on the relative pressures of ethanol and propionitrile. More importantly, the rate constants derived from the decay curves of protonated propionitrile were independent of the pressure of either ethanol or propionitrile, as expected.

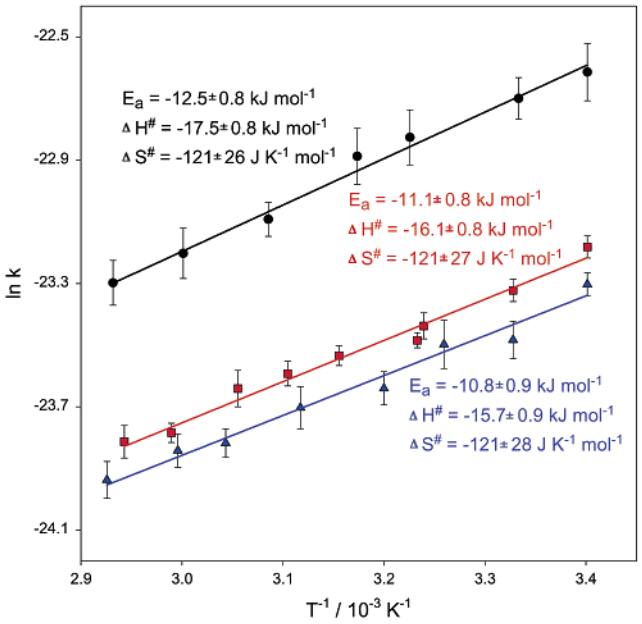

Figure 5. Arrhenius plots for the S_N2 reactions between protonated ethanol and ethanol (red squares), protonated propionitrile and ethanol (black circles), and protonated *n*-propanol and *n*-propanol (blue triangles).

TABLE 2: Rate Constants for the Ethyl Cation Exchange Reaction between Ethanol and Protonated Propionitrile

temp, K	rate constant[a]	temp, K	rate constant[a]
294	15.1 ± 1.4	324	9.4 ± 0.5
300	13.9 ± 0.9	333	8.4 ± 0.7
310	12.2 ± 1.1	341	7.6 ± 0.6
315	11.5 ± 1.1		

[a] Rate constants in units of 10^{-11} cm^3 s^{-1}.

TABLE 3: Rate Constants[a] and Barrier Heights[b] for Methyl Cation Transfer Reactions

reaction	Fridgen/ McMahon[c]	McCormack/ Mayer	Meot-Ner/ Karpas
$CH_3CNH^+ + CH_3OH$	3.5 (−16.5)	4.6[d] (+13)	2.7[f]
$CH_3OH_2^+ + CH_3OH$	11.1 (−16.9)	11[e] (+1)	10.8[g]

[a] Units of 10^{-11} cm^3 s^{-1}. [b] In parentheses and in units of kJ mol^{-1}. [c] Reference 5. [d] Reference 9. [e] Reference 8. [f] Reference 20. [g] Reference 16.

The rate constants for ethyl cation exchange between protonated propionitrile and ethanol were significantly greater than those for the reaction of the protonated ethanol with ethanol ranging from 15.1 × 10^{-11} to 7.6 × 10^{-11} cm^3 s^{-1} at 294 and 341 K, respectively (see Table 2). Although there have been no rate constants measured for this particular reaction in the past, it is worth noting that McCormack and Mayer have measured rate constants for the ethyl cation transfer reactions in the quadrupole ion trap, specifically between protonated acetonitrile and ethanol (39 × 10^{-11} cm^3 s^{-1})[9] and between protonated ethanol and ethanol (14 × 10^{-11} cm^3 s^{-1}),[8] which shows that ethyl cation transfer is considerably faster in the nitrile system. This is in contrast to the methyl cation transfer reactions. The rate constants for methyl cation transfer between protonated methanol and methanol and between protonated acetonitrile and methanol have been measured by three different groups and those for the latter reaction were larger in all three cases (see Table 3).

It is not totally surprising that the rates for the methyl cation reactions are different given that the barrier height for the

protonated acetonitrile/methanol reaction is higher than that for the protonated methanol/methanol reaction (barrier heights are given in parentheses in Table 3). The barrier heights obtained by McCormack and Mayer[8,9] in an ion trap for these two reactions are significantly higher than those determined previously by us.[5] Through the use of eqs 6 and 9, the preexponential factors and the entropy of activation for the two methyl cation exchange reactions can be obtained. With the use of the values for the barrier height and rate constants that McCormack and Mayer obtained (Table 3), values for $\Delta S^{\ddagger}$ of -78 and -45 J K^{-1} mol^{-1} for reactions A and B (see Table 3), respectively, are determined. The difference in these two values (33 J K^{-1} mol^{-1}) seems unusually large for reactions that are so similar in nature. Furthermore, both values seem to be too positive for these types of reactions.

The Arrhenius plot for the ethyl cation transfer reaction between protonated propionitrile and ethanol is shown in Figure 5. The E_a and $\Delta H^{\ddagger}$ were determined to be -12.5 ± 0.8 and -17.5 ± 0.8 kJ mol^{-1}, respectively, from the slope of the Arrhenius plot. These values are slightly lower than those obtained for the protonated ethanol/ethanol reaction. Mayer and McCormack[9] and Ochran et al.[7] estimated barrier heights for the ethyl cation transfer reaction between protonated acetonitrile and ethanol to be -10 ± 10 and -22 ± 10 kJ mol^{-1}, respectively.

The entropy of activation was determined to be -121 ± 26 J K^{-1} mol^{-1}, which is the same as that for the protonated ethanol/ethanol reaction. Given that the entropies of activation are virtually identical and that the barrier for the protonated propionitrile/ethanol reaction is lower, it is not surprising that the rate constants are higher.

$CH_3CH_2CH_2OH_2^+ + CH_3CH_2CH_2OH$. The major products observed in the reaction of protonated *n*-propanol with *n*-propanol were protonated di-*n*-propyl ether (*m*/*z* 103) and the proton-bound dimer of *n*-propanol. The ratios of these two products were dependent on the conditions of temperature and pressure under which the reaction was carried out. For example, the proton-bound dimer was favored, albeit only slightly, at higher pressures of *n*-propanol and at the lowest temperatures. At increased temperatures or at lower pressures, the S_N2 channel dominated. These observations are consistent with the nascent proton-bound dimer being stabilized more efficiently at higher pressures because of the increased collision frequency. As well, the unimolecular dissociation of the nascent proton-bound dimer is more affected by temperature than the S_N2 reaction. Also observed were two minor products. A small amount of *m*/*z* 101 was observed, which is presumably due to loss of H_2 from nascent protonated di-*n*-propyl ether. The reaction of *n*-propanol with protonated *n*-propanol to form H_2O, H_2, and *m*/*z* 101 is exothermic by approximately 30 kJ mol^{-1}, according to B3LYP/6-31+G* calculations, if *m*/*z* 101 is O-propylated propanal,

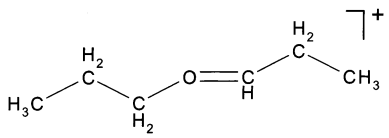

O-propylated propanal cation (m/z 101)

The small amount of *m*/*z* 101 observed during the course of these experiments (~5%) is quite likely due to the presence of a substantial barrier to loss of H_2. As well, a small amount of the mixed proton-bound dimer of di-*n*-propyl ether and *n*-propanol was observed and is discussed in detail elsewhere.[12]

The rate constant for *n*-propyl cation transfer between *n*-propanol and protonated *n*-propanol, forming protonated di-*n*-propyl ether was found to be 7.6×10^{-11} cm^3 s^{-1} at 294 K and decreased to 4.0×10^{-11} cm^3 s^{-1} at 342 K (Table 4). Karpas and Meot-Ner[16] measured the rate constant for this reaction in an ICR spectrometer and obtained a slightly higher value, 10.3×10^{-11} cm^3 s^{-1}, at ambient temperature. In contrast, McCormack and Mayer[8] measured this rate constant to be almost an order of magnitude larger, 63×10^{-11} cm^3 s^{-1}, in a quadrupole ion trap. The most likely reason for the discrepancy among the values can be attributed to calibration factors for the pressure of neutral *n*-propanol. Although we cannot say which value is more dependable, the calibration factor will have no effect on the activation energies derived from our temperature-dependent rate constants but it does have an effect the value of $\Delta S^{\ddagger}$ obtained (see below).

TABLE 4: Rate Constants for the *n*-Propyl Cation Exchange Reaction between *n*-Propanol and Protonated *n*-Propanol

temp, K	rate constant[a]	temp, K	rate constant[a]
294	7.6 ± 0.3	321	5.1 ± 0.4
301	6.3 ± 0.4	329	4.5 ± 0.2
307	6.2 ± 0.5	334	4.4 ± 0.2
313	5.4 ± 0.3	342	4.0 ± 0.2

[a] Rate constants in units of 10^{-11} cm^3 s^{-1}.

The Arrhenius plot for the *n*-propanol/ protonated *n*-propanol S_N2 reaction is given in Figure 5. The E_a and $\Delta H^{\ddagger}$ were determined to be -10.8 ± 0.9 and -15.7 ± 0.9 kJ mol^{-1}, respectively, which are only slightly lower than the corresponding values for the ethyl cation transfer between protonated ethanol and ethanol. The barrier estimated by McCormack and Mayer[8] was -22 ± 8 kJ mol^{-1}, which is in reasonable agreement with our purely experimental value.

The entropy of activation for the *n*-propyl cation transfer reaction was also found to be -121 ± 28 J K^{-1} mol^{-1}. If our calibration factor of 1.25 for the pressure of neutral *n*-propanol is incorrect, this would affect the rate constants. The measured rate constants for the *n*-propyl cation transfer between *n*-propanol and protonated *n*-propanol have the largest discrepancy between measurements from different groups. Calibration factors of 0.95 or 0.16 would be required to bring our measured rate constants into agreement with those measured by Karpas and Meot-Ner[8] or McCormack and Mayer,[8] respectively. This would decrease our value of $\Delta S^{\ddagger}$ to -119 or -104 J K^{-1} mol^{-1}. These values are still within our determined experimental error, but the latter is lower than would be expected for this type of reaction. Changing the calibration factor would not affect the determination of the activation energies.

5.2. Comparison of Experimental and Calculated Thermochemistry. The experimental and calculated values of $\Delta H^{\ddagger}$ for the alkyl cation transfer reactions studied by us to date are tabulated in Table 5. G3(MP2)[17] calculations have been carried out on the three methyl cation transfer reactions to compare with the MP2/6-31+G(d)//B3LYP/6-31+G(d) calculations, which are reported for the ethyl and *n*-propyl cation transfer reactions. For the three methyl cation transfer reactions, the G3(MP2) and MP2/6-31+G(d)//B3LYP/6-31+G(d) calculated energy barriers are in excellent agreement. More significantly, these calculations are in excellent agreement with the experimentally determined energy barriers. This agreement with the G3(MP2) and experimental barriers provides confidence in the MP2/6-31+G(d)//B3LYP/6-31+G(d) calculations for the ethyl and *n*-propyl cation transfer reactions. As seen in Table 5, the calculated and experimental values of the energy barriers for the ethyl and *n*-propyl cation transfer reactions are in excellent agreement as well.

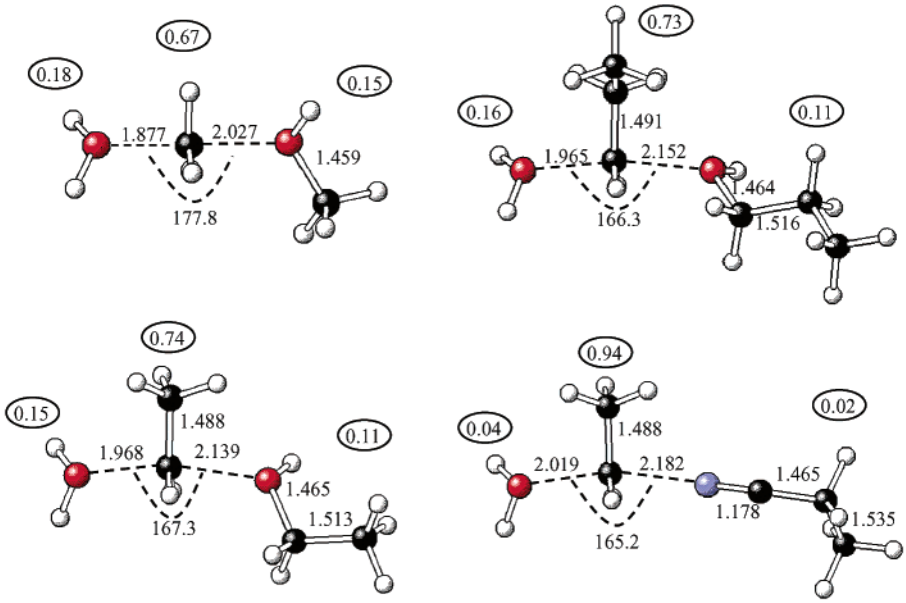

Figure 6. MP2/6-31+G* calculated transition-state structures for the two ethyl cation transfer reactions and the *n*-propyl cation transfer reaction, as well as the methyl cation transfer reaction between protonated methanol and methanol.

TABLE 5: Calculated and Experimental Energy Barriers[a] for S_N2 Alkyl Cation Transfer Reactions

	MP2/6-31+G*// B3LYP/6-31+G*	G3(MP2)	experiment
Methyl Cation Transfer Reactions (Reaction with Neutral Methanol)			
$CH_3OH_2^+$	−22.7	−22.4	−16.9 ± 0.6[b]
CH_3CNH^+	−17.9	−17.8	−16.5 ± 0.6[b]
CH_3CHOH^+	−23.7	−15.4	−18.4 ± 0.7[b]
Ethyl Cation Transfer Reactions (Reaction with Neutral Ethanol)			
$CH_3CH_2OH_2^+$	−20.2		−16.1 ± 0.8
$CH_3CH_2CNH^+$	−18.1		−17.5 ± 0.8
n-Propyl Cation Transfer Reactions (Reaction with Neutral *n*-Propanol)			
$CH_3(CH_2)_2OH_2^+$	−20.7		−15.7 ± 0.9

[a] In units of kJ mol^{-1}. [b] Experimental values for methyl cation transfer from ref 5.

TABLE 6: Experimental and Calculated Entropy Differences[a] Between Products and the Transition State for Alkyl Cation Transfer Reactions

	B3LYP/6-31+G*	experiment
Methyl Cation Transfer Reactions (Reaction with Neutral Methanol)		
$CH_3OH_2^+$	−133	−121 ± 20[b]
CH_3CNH^+	−115	−130 ± 20[b]
CH_3CHOH^+	−126	−144 ± 17[b]
Ethyl Cation Transfer Reactions (Reaction with Neutral Ethanol)		
$CH_3CH_2OH_2^+$	−121	−121 ± 27
$CH_3CH_2CNH^+$	−116	−121 ± 26
n-Propyl Cation Transfer Reactions (Reaction with Neutral *n*-Propanol)		
$CH_3(CH_2)_2OH_2^+$	−126	−121 ± 28

[a] In units of J K^{-1} mol^{-1}. [b] Experimental values for methyl cation transfer from ref 5.

The structures and Mulliken charges for the transition states calculated at the MP2/6-31+G(d) level are shown in Figure 6. The charge in each of the transition states is predominantly on the alkyl group that is being transferred, and in the reaction involving propionitrile, the ethyl group being transferred bears almost all of the charge. It is apparent that, prior to alkyl cation transfer, an isomerization is required from the proton-bound dimer to produce an alkyl-bound isomer in which the oxygen of the neutral alcohol is complexed to the alkyl group of the protonated alcohol. The calculated energy profiles for the methanol/protonated methanol reaction have been presented previously.[5,18,19] In the case of the reaction between protonated propionitrile and ethanol, the isomerization from the proton-bound dimer also includes a proton transfer to ethanol, which has a lower proton affinity than propionitrile. Calculated energy profiles for the methyl and ethyl cation exchanges between protonated acetonitrile and methanol[5] and ethanol,[7] respectively, have been reported previously. In each of these studies, it was shown that the calculated energy barriers for isomerization of the proton-bound dimers to the alkyl-bound isomers are significantly lower than the barrier to alkyl cation transfer. The bottleneck for alkyl cation transfer, therefore, is not isomerization of the proton-bound dimer.

It is interesting that the entropy differences measured between the reactants and the barriers for alkyl cation transfer for those reactions reported here are all 121 J K^{-1} mol^{-1} (± approximately 27 J K^{-1} mol^{-1}). The calculated entropy differences are given in Table 6 along with the experimental values for the methyl, ethyl, and *n*-propyl cation transfer reactions studied. In all cases, the calculated entropy differences agree quite well with the experimental entropy differences.

5.3 Comparison of Methyl, Ethyl, and *n*-Propyl Cation Transfer. It also may be instructive to compare the energy barriers for the methyl, ethyl, and *n*-propyl cation reactions forming the protonated dimethyl, diethyl, and di-*n*-propyl ethers. The experimental values of the barrier heights increase slightly over this series going from −16.9 ± 0.6 to −16.1 ± 0.8 to −15.7 ± 0.9 kJ mol^{-1}. Within the reported uncertainty, the energy barriers are, however, roughly the same. The experimental values for the barrier heights agree quite well with the calculated values (see Table 5), which also show very little variation for these three reactions. The structures of the transition states (Figure 6) also show very little variation with respect to the bond distances between the transferring alkyl group and the leaving and accepting sites. Also the average charge on the

transferring alkyl groups is fairly constant for the methyl, ethyl, and *n*-propyl cation exchange reactions.

6. Conclusions

Energy barriers for three alkyl cation transfer reactions have been experimentally determined. The experimental values have been shown to be in excellent agreement with MP2/6-31+G*//B3LYP/6-31+G* calculations. Furthermore, the differences in entropy between the reactants and the transition state were all shown to be approximately 121 J K^{-1} mol^{-1}, which also agrees with the theoretical values. The experimental energy barriers for methyl, ethyl, and *n*-propyl cation transfer are virtually identical within experimental uncertainty. The ethyl cation transfer reaction was shown to be the dominant route for both of the reactions of ethanol with protonated propionitrile and protonated *n*-propanol. The *n*-propyl cation transfer reaction of *n*-propanol with protonated *n*-propanol competes with the radiative association reaction giving a roughly 50:50 mixture of di-*n*-propyl ether and the proton-bound dimer.

Acknowledgment. The financial support of the Research Grants Program of the Natural Sciences and Engineering Research Council of Canada (NSERC) is acknowledged. T.D.F. gratefully acknowledges the Posdoctoral Fellowship granted by NSERC.

References and Notes

(1) For example, see these references and references therein. (a) Cheng, Y.-W.; Dunbar, R. C. *J. Phys. Chem.* **1995**, *99*, 10802. (b) Ryzhov, V.; Yang, Y.-C.; Klippenstein, S. J.; Dunbar, R. C. *J. Phys. Chem. A* **1998**, *102*, 8865. (c) Petrie, S.; Dunbar, R. C. *J. Phys. Chem. A* **2000**, *104*, 4480.

(2) Fridgen, T. D.; McMahon, T. B. *J. Phys. Chem. A* **2001**, *105*, 1011.

(3) (a) Klippenstein, S. J.; Yang, Y. C.; Ryzhov, V.; Dunbar, R. C. *J. Chem. Phys.* **1996**, *104*, 4502. (b) Dunbar, R. C. *J. Phys. Chem. A* **1998**, *102*, 8946. (c) Gapeev, A.; Dunbar, R. C. *J. Phys. Chem. A* **2000**, *104*, 4084.

(4) Fridgen, T. D.; McMahon, T. B. *J. Am. Chem. Soc.* **2001**, *123*, 3980.

(5) Fridgen, T. D.; Keller, J. D.; McMahon, T. B. *J. Phys. Chem. A* **2001**, *105*, 3816.

(6) Mayer, P. M. *J. Phys. Chem. A* **1999**, *103*, 3687.

(7) Ochran, R. A.; Annamalai, A.; Mayer, P. M. *J. Phys. Chem. A* **2000**, *104*, 8505.

(8) McCormack, J. A. D.; Mayer, P. M. *Int. J. Mass Spectrom.* **2001**, *207*, 183.

(9) McCormack, J. A. D.; Mayer, P. M. *Int. J. Mass Spectrom.* **2001**, *207*, 195.

(10) Su, T.; Chesnavich, W. J. *J. Chem. Phys.* **1982**, *76*, 5183.

(11) Frisch, M. J.; Trucks, G. W.; Schlegel, H. B.; Scuseria, G. E.; Robb, M. A.; Cheeseman, J. R.; Zakrzewski, V. G.; Montgomery, J. A., Jr.; Stratmann, R. E.; Burant, J. C.; Dapprich, S.; Millam, J. M.; Daniels, A. D.; Kudin, K. N.; Strain, M. C.; Farkas, O.; Tomasi, J.; Barone, V.; Cossi, M.; Cammi, R.; Mennucci, B.; Pomelli, C.; Adamo, C.; Clifford, S.; Ochterski, J.; Petersson, G. A.; Ayala, P. Y.; Cui, Q.; Morokuma, K.; Malick, D. K.; Rabuck, A. D.; Raghavachari, K.; Foresman, J. B.; Cioslowski, J.; Ortiz, J. V.; Stefanov, B. B.; Liu, G.; Liashenko, A.; Piskorz, P.; Komaromi, I.; Gomperts, R.; Martin, R. L.; Fox, D. J.; Keith, T.; Al-Laham, M. A.; Peng, C. Y.; Nanayakkara, A.; Gonzalez, C.; Challacombe, M.; Gill, P. M. W.; Johnson, B. G.; Chen, W.; Wong, M. W.; Andres, J. L.; Head-Gordon, M.; Replogle, E. S.; Pople, J. A. *Gaussian 98*, revision A.7; Gaussian, Inc.: Pittsburgh, PA, 1998.

(12) Fridgen, T. D.; McMahon, T. B. *J. Phys. Chem. A* **2002**, *106*, 1576.

(13) Lias, S. G.; Bartmess, J. E.; Liebman, J. F.; Holmes, J. L.; Levin, R. D.; Mallard, W. G. *J. Phys. Chem. Ref. Data* **1988**, *17*, Suppl. 1.

(14) Øiestad, E. L.; Øiestad, Å. M. L.; Skaane, H.; Ruud, K.; Helgaker, T.; Uggerud, E. *Eur. Mass Spectrom.* **1995**, *1*, 121.

(15) McMahon, T. B.; Beauchamp, J. L. *J. Phys. Chem.* **1977**, *81*, 593.

(16) Karpas, Z.; Meot-Ner, M. *J. Phys. Chem.* **1989**, *93*, 1859.

(17) Curtiss, L. A.; Redfern, P. C.; Raghavachari, K.; Rassolov, V.; Pople, J. A. *J. Chem. Phys.* **1999**, *110*, 4703.

(18) Bouchoux, G.; Choret, N. *Rapid Commun. Mass Spectrom.* **1997**, *11*, 1799.

(19) Ragavachari, K.; Chandrasekhar, J.; Burnier, R. C. *J. Am. Chem. Soc.* **1984**, *10*, 3124.

(20) Meot-Ner, M.; Karpas, Z. *J. Phys. Chem.* **1986**, *90*, 2206.